Article

Synthesis and initial biological evaluation of boron-containing prostate specific membrane antigen ligands for treatment of prostate cancer using boron neutron capture therapy

Sinan Wang, Charles Blaha, Raquel Santos, Tony Huynh, Thomas R. Hayes, Denis R. Beckford Vera, Joseph E Blecha, Andrew S Hong, Miko Fogarty, Thomas A Hope, David R Raleigh, David M. Wilson, Michael J. Evans, Henry F. VanBrocklin, Tomoko Ozawa, and Robert R. Flavell

Mol. Pharmaceutics, **Just Accepted Manuscript** • DOI: 10.1021/acs.molpharmaceut.9b00464 • Publication Date (Web): 05 Aug 2019

Synthesis and initial biological evaluation of boron-containing prostate specific membrane antigen ligands for treatment of prostate cancer using boron neutron capture therapy

Sinan Wang[†], Charles Blaha[‡], Raquel Santos[§], Tony Huynh[†], Thomas R. Hayes[†], Denis R. Beckford-Vera[†], Joseph E. Blecha[†], Andrew S. Hong[†], Miko Fogarty[§], Thomas A. Hope[†], David R. Raleigh[§,I], David M. Wilson[†], Michael J. Evans[†], Henry F. VanBrocklin[†], Tomoko Ozawa[§], Robert R. Flavell[*,†]

[†]Department of Radiology and Biomedical Imaging, University of California, San Francisco, California, USA.
[‡]Department of Bioengineering and Therapeutic Sciences, University of California, San Francisco, California, USA.
[§]Department of Neurological Surgery, University of California, San Francisco, California, USA.
[I]Departments of Radiation Oncology, University of California, San Francisco, California, USA.

ABSTRACT:

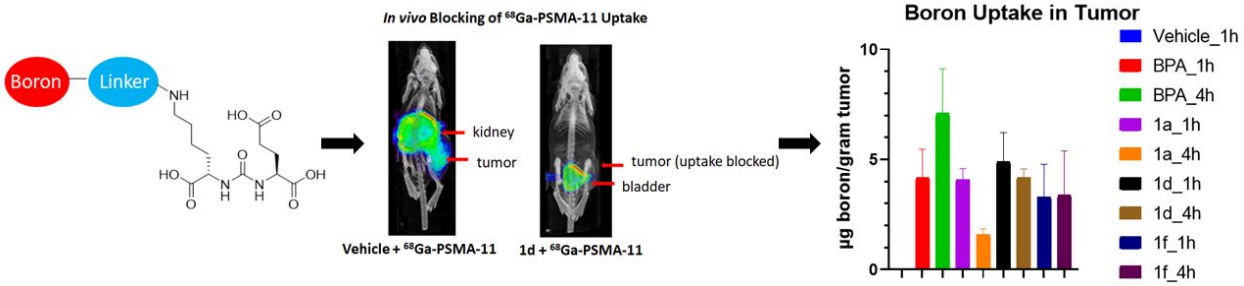

Boron neutron capture therapy (BNCT) is a therapeutic modality which has been used for the treatment of cancers, including brain and head and neck tumors. For effective treatment via BNCT, efficient and selective delivery of a high boron dose to cancer cells is needed. Prostate specific membrane antigen (PSMA) is a target for prostate cancer imaging and drug delivery. In this study, we conjugated boronic acid or carborane functional groups to a well-established PSMA inhibitor scaffold to deliver boron to prostate cancer cells and prostate tumor xenograft models. Eight boron-containing PSMA inhibitors were synthesized. All of these compounds showed strong binding affinity to PSMA in a competition radioligand binding assay (IC_{50} from 555.7 nM-20.3 nM). Three selected compounds **1a**, **1d** and **1f** were administered to mice, and their *in vivo* blocking of ^{68}Ga-PSMA-11 uptake was demonstrated through a positron emission tomography (PET) imaging and biodistribution experiment. Biodistribution analysis demonstrated boron uptake of 4-7 μg/gram in 22Rv1 prostate xenograft tumors and similar tumor/muscle ratios compared to the ratio for the most commonly used BNCT compound, 4-

borono-L-phenylalanine (BPA). Taken together, this data suggest a potential role for PSMA targeted BNCT agents in prostate cancer therapy following suitable optimization.

KEYWORDS: *Boron neutron capture therapy (BNCT), prostate cancer, prostate specific membrane antigen (PSMA) inhibitor, carborane, boron uptake*

■ INTRODUCTION

Boron neutron capture therapy is a cancer treatment method based on the selective uptake of boron-containing drugs into cancer cells over normal cells, followed by selective neutron beam exposure to the cancerous regions.[1,2,3] This irradiation initiates the emission of cytotoxic alpha particles and lithium ions. The released high linear energy transfer (LET) α-particles can travel a distance of only around 9 μm in tissue, which is approximately the diameter of a cell. Therefore, their short-range cytotoxicity can significantly improve tumor control with concomitant sparing of the surrounding normal tissues.[4,5] This therapeutic modality has been successfully used for treatment of patients with primary brain and head and neck tumors.[6,7,8] Clinically used BNCT reagents include 4-borono-L-phenylalanine (BPA) and sodium borocaptate (BSH).[9,10,11] However, due to various limitations including relatively low target to background ratio binding of boron-labeled therapeutic agents, BNCT has yet to emerge as a standard of care treatment modality for most cancer types.

Prostate cancer (PCa) is one of the most prevalent noncutaneous cancer in men.[12,13] Prostate specific membrane antigen, also known as glutamate carboxypeptidase II (GCPII) or N-acetyl-L-aspartyl-L-glutamate peptidase, is a cell surface enzyme which is highly expressed on prostate cancer cells.[14] Recently, urea based inhibitor agents targeting the enzymatic domain of PSMA have been developed for both imaging and therapy of prostate cancer.[15,16,17,18] Therapy with radionuclides has been demonstrated using ^{177}Lu and ^{225}Ac, which exhibit successful tumor control but also have side effects including xerostomia and bone marrow suppression.[19,20] PSMA targeted therapeutics and imaging agents have been extended beyond radionuclides, including nanoparticles and antibody drug conjugates.[21,22,23]

The high target to background ratio of PSMA targeted imaging and therapeutic agents, coupled with the high efficacy of BNCT, suggest the potential for boron labeled PSMA targeting agents as effective BNCT agents. In principle, this approach could combine the benefit of high target to background ratio of PSMA directed therapeutics with the spatial localization offered by a neutron beam. Therefore, this approach could be used for treatment of oligometastatic prostate cancer, potentially the minimizing off target side effects of radionuclides including xerostomia and bone marrow suppression. Boron labeled PSMA targeting agents have been reported, their binding to the enzyme characterized, and initial biodistribution studied using radioiodinated derivatives.[24,25] However, these studies did not determine the degree of boron uptake in tumors,

which is necessary to predict therapeutic efficacy. We hypothesize that by using boron-containing target-specific molecules, the localized and enhanced expression of PSMA on PCa cells in comparison to normal tissue could enable preferential and adequate delivery of boron to PCa for BNCT. We designed a series of boron labeled agents targeting PSMA including three components – a urea-based PSMA binding group, a linker moiety, and a substituent containing one, ten, or twenty boron atoms (Figure 1). In this study, we report the synthesis of a series of boron-labeled agents targeting PSMA, and their initial *in vitro* and *in vivo* evaluation in biodistribution assays.

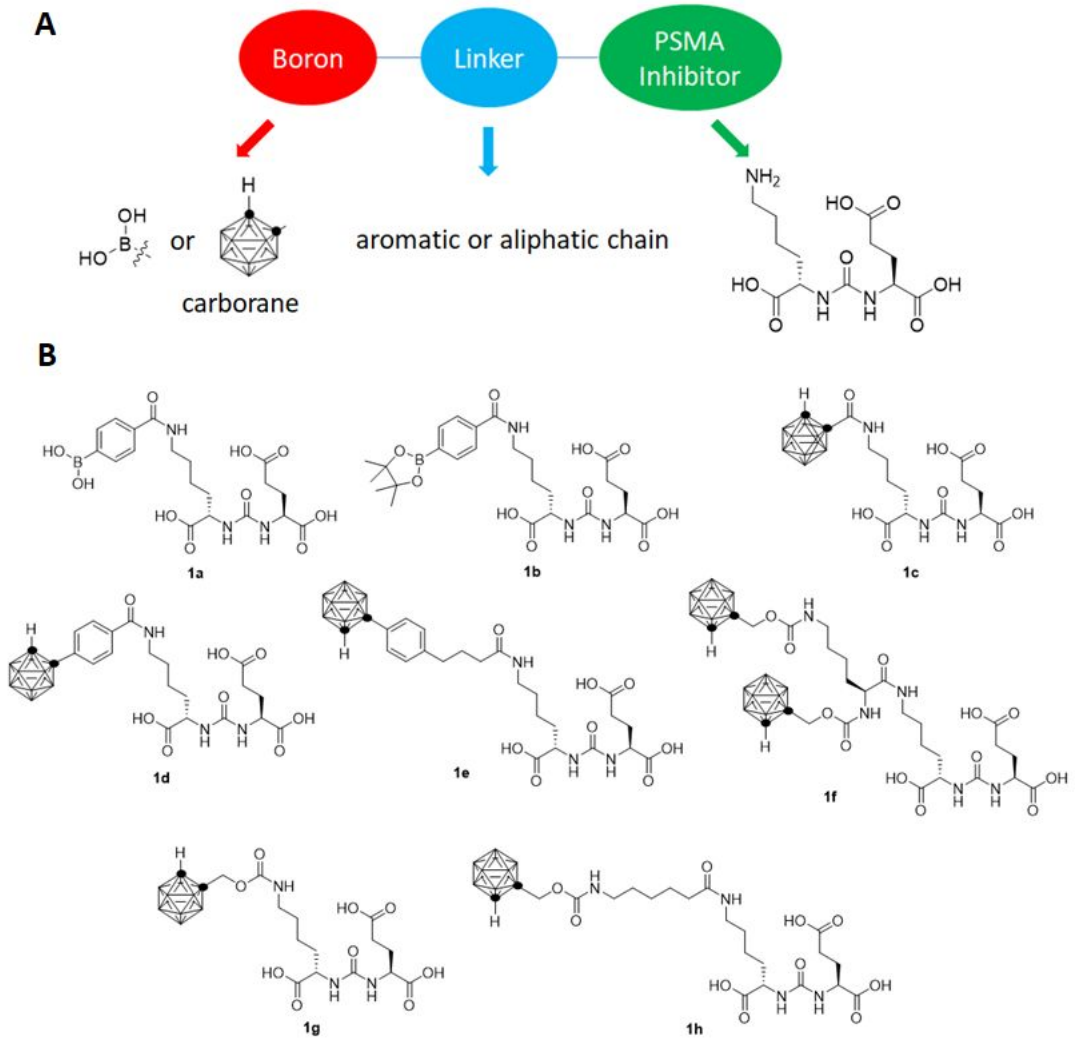

Figure 1. (A) The design of boron labeled PSMA targeted agents includes a urea based inhibitory element, connected to a boron containing substituent via a linker moiety. (B) Structures of boron labeled PSMA agents evaluated in this study.

■ EXPERIMENTAL SECTION

2.1. Materials.

o-Carborane was purchased from Boron Specialties (PA, U.S.A.). Decaborane and all other chemicals were purchased from Sigma-Aldrich (MO, U.S.A.). RPMI-1640 medium, Fetal bovine serum (FBS) and penicillin-streptomycin solutions were purchased from Life Technologies (NY, U.S.A.).

2.2 Chemistry.

Details for the synthesis and characterizations of all compounds are provided in the supplementary information.

2.3 Cell Culture

The PSMA-expressing human prostate cancer cell line 22Rv1 was obtained from ATCC. 22Rv1 cells were maintained in RPMI-1640 medium supplemented with 10% fetal bovine serum (FBS), 100 units of penicillin and 100 μg/mL streptomycin in a humidified incubator at 37 ^{o}C and 5% CO_2. Cells were removed from flasks for passage or for transfer to 48-well assay plates by incubating them with 0.25% trypsin.

2.4 IC_{50} Measurement

IC_{50} values of the boron-containing compounds **1a-h** were determined by screening in a competition radioligand binding assay against ^{68}Ga-PSMA-11. ^{68}Ga-PSMA-11 was synthesized as previously reported using at ^{68}Ge/^{68}Ga generator and a manual synthesis model, using 5 μg precursor yielding approximately 10-35 mCi per batch.[26] 2-(phosphonomethyl) pentanedioic acid (PMPA) is a known PSMA inhibitor and has been chosen as a positive control.[27] 22Rv1 cells were plated in a 48-well plates (250 μL/well) 48 h before testing (triplet) in RPMI1640 medium supplemented with 10% fetal bovine serum. The cell number was about 250,000 per well when the assay was performed. The growth medium was removed and washed with PBS for three times. Various concentrations (0.01-100000 nM) of the tested compounds in serum free RPMI1640, together with 10 μCi (5 ng) of ^{68}Ga-PSMA-11, were added to cells. The cells were incubated in this buffer for 1 h at 37^{o} C. Then the radioactive medium was removed by pipette, and cells were washed by PBS twice, and 250 μL of 5N NaOH was added to lyse the cells. The lysate was transferred to small vials, and the bound radioactivity was counted using a Hidex

gamma counter. IC_{50} values were determined by nonlinear regression using GraphPad Prism software (GraphPad Software).

2.5 Log P Measurement

Log P measurements were made using the "shake-flask" method[25,28]. The ICP matrix was prepared using 2% H_2SO_4, 2% HNO_3 and 0.3% triton in Millipore water. 50 µL of 1 mM compound in PBS (pH = 7.4) was added to each of three vials containing 50 µL of 1-octanol. The vials were shaken on a vortex mixer for 10 min, followed by centrifugation for a further 10 min. Aliquot (30 µL) of each PBS and octanol layer were transferred to 15 mL Falcon tubes and diluted to 10 mL with ICP matrix buffer or 0.3 mL of EtOH and 9.7 mL of ICP matrix buffer respectively. The boron content was measured by Inductively Coupled Plasma Optical-Emission Spectrometry (ICP-OES, Thermo Scientific iCAP 7000 series). Log P values were calculated as Log{[boron content per mL(1-octanol)]/[boron content per mL(buffer)]}.

2.6 Internalization Studies

When cells reached 70% confluency in a T75 flask, medium was removed, and the cells were washed twice with PBS. 20 mL 100 µM compound in serum free RPMI 1640 was added and the cells were incubated at 37 ^oC for 1 hour. The medium was removed and the cells were washed with PBS twice. The cells were detached with 0.25% trypsin solution. The cells were washed three times with PBS and then treated with a solution of 50 mM glycine and 100 mM NaCl at pH 3 for 2 min at 37 °C and 5% CO_2. Cells were then centrifuged (3 min at 12,000 rpm), and the supernatant was collected. This treatment was repeated two additional times, and the combined supernatants were diluted to 10 mL with ICP matrix. The pellet was digested by 400 µL 1:1 H_2SO_4/HNO_3 mixture overnight, then diluted to 10 mL by ICP matrix. The boron content was measured by Inductively Coupled Plasma Optical-Emission Spectrometry (ICP-OES, Thermo Scientific iCAP 7000).

2.7 Inoculation of Mice with Xenograft

All animal studies were conducted according to an Institutional Animal Care & Use Program (IACUC) approved protocol. Five to six weeks old, male athymic mice (nu/nu, homozygous; Jackson Laboratories), housed in aseptic conditions, received subcutaneous tumor cell inoculation, as approved by the University of California, San Francisco Institutional Animal Care and Use Committee. In brief, 5 million 22Rv1 cells in a 200 µL 1:1 mixture of complete medium and matrigel (Fisher Scientific, IL) was injected in the left thigh of the animals. All

mice were subjected to undergo PET imaging as well as biodistribution analysis when the tumor reached a size of 300 - 500 mm^3.

2.8 Serum protein binding assay

25 µl of 1 mM compound in PBS was added to 0.5 ml mouse serum. The mixture was vortexed for 5 mins and incubated at 37 ^oC for 30 mins. Then 0.5 ml acetonitrile was added to precipitate the protein. The mixture was then centrifuged (3 min at 12,000g), and the supernatants and pellet were collected respectively. ICP matrix was prepared by 2% H_2SO_4, 2% HNO_3, 0.3% triton in millipore water. The supernatants were diluted to 10 ml by ICP matrix. The pellet was digested by 400 µl 1:1 H_2SO_4/HNO_3 mixture overnight, then diluted to 10 ml by ICP matrix. The boron content was measured by ICP-OES.

2.9 Toxicity Test

Cell toxicity assay was performed using a CellTiter-Glo kit to measure the viability of cells after incubating with various concentrations of compounds. 22Rv1 cells were plated in a 96-well plates (100 µL/well) 48 h before testing (triplet) in RPMI1640 medium supplemented with 10% fetal bovine serum. The growth medium was removed and washed with PBS for three times. Various concentrations (0.01-100000 nM) of the tested compounds in PBS and blank were added to cells. The cells were incubated in this buffer for 4 h at 37^o C. Then 100 µL of CellTiter-Glo buffer was added to each well. The mixture was incubated at room temperature for 15 minutes and the luminescence was measured using a luminometer.

For animal toxicity experiments, non-tumor bearing male athymic mice were administered graded intraperitoneal doses of the selected boronated compounds to determine the maximum tolerated dose (5 mg/mouse, 7.5 mg/mouse, 15 mg/mouse or 30mg/mouse), and were monitored for 24 hours. Each testing group contained two mice. If animals showed physical symptoms as outlined by our IACUC guidelines such as loss of activity, animals were euthanized.

2.10 *In Vivo* PET Imaging Studies.

Approximately three weeks after implantation, animals with tumors reaching 300-500 mm^3 were anesthetized by isoflurane inhalation and were administered 200 µL of PBS, compound **1a (**30 mg/mouse in 200 µL of PBS**)**, **1d** (5 mg/mouse in a mixture of 40 µL of DMSO and 160 µL of PBS) or compound **1f** (7.5 mg/mouse in a mixture of 40 µL of DMSO and 160 µL of PBS) through a single intraperitoneal injection. BPA (5 mg/mouse) was administered to mice through oral gavage due to its low solubility in buffer. Approximately 15 minutes after the administration

of these compounds, 100-150 μCi (3.70-5.55 MBq, 50 – 75 ng) of ^{68}Ga-PSMA-11 was administered through tail vein injection. The animals were imaged with 10 min acquisition by a microPET/CT imaging system (Inveon, Siemens, Germany) at 1 h post injection of the first administration. PET imaging data were acquired in list mode and reconstructed with the iterative OSEM 2-D reconstruction algorithm provided by the manufacturer. Imaging data were viewed and processed using open source Amide software.

2.11 Biodistribution Studies.

The 22Rv1 tumor bearing mice were sacrificed at the 1 hour or 4 hour time points post injection of ^{68}Ga-PSMA-11. Blood was collected by cardiac puncture. Major organs (brain, bone, heart, kidney, liver, lung, muscle, pancreas, salivary, skin, spleen and subcutaneous tumor) were harvested, weighed, and counted in an automated gamma counter (Hidex). The percent injected dose per gram of tissue (% ID/g) was calculated by comparison with standards of known radioactivity.

2.12 Organ Digestion and ICP Mass

Tissue samples were digested for 2 days at room temperature in 1 mL of a 1:1 mixture of concentrated sulfuric and nitric acids. After digestion, 1.5 mL of a 5 % Triton X-100 solution in water was added to each sample. The samples were then sonicated for 90 min. 1 mL of the sample solution was transferred to a 15 mL centrifuge tube and diluted to 10 mL with ICP matrix. The samples were processed for boron analysis by ICP-OES.

■ RESULTS

3.1 Synthesis of Compound 1a-1f.

The syntheses of compounds **1a-f** are outlined in scheme 1. Various boron-containing activated esters were coupled to a common synthetic intermediate **12** to yield the final products. Starting materials **2a** and **2b** are commercially available. Starting materials **2c**[24], **3**[29], **5**[30], **9**[31], **12**[32] and reagent $B_{10}H_{12}(MeCN)_2$[31] were obtained following known literature procedures. Briefly, compound **3** was reacted with $B_{10}H_{12}(MeCN)_2$ followed by deprotection to generate intermediate **2d.** Sonogashira coupling of compound **5** with trimethylsilyl acetylene followed by a deprotection formed intermediate **7**. Reacting **7** with $B_{10}H_{12}(MeCN)_2$ followed by deprotection gave carborane containing intermediate **2e.** Mixing compound **9** with 4-nitrophenyl chloroformate produced carbonate **10**. Then **10** was reacted with *L*-lysine tert-butyl ester hydrochloride followed by deprotection to give di-carborane containing intermediate **2f**. Each of

the obtained boron containing intermediates **2a-f** was mixed with *N,N′*-Dicyclohexylcarbodiimide (DCC) and *N*-Hydroxysuccinimide (NHS) in THF and stirred overnight, the precipitation was removed by filtration. Then, compound **12** was added to the solution, the mixture was stirred for 24 hours. After purification by chromatography, each of compound **13a-f** was reacted with TFA in DCM to remove the protecting groups, yielding the final products **1a-f**.

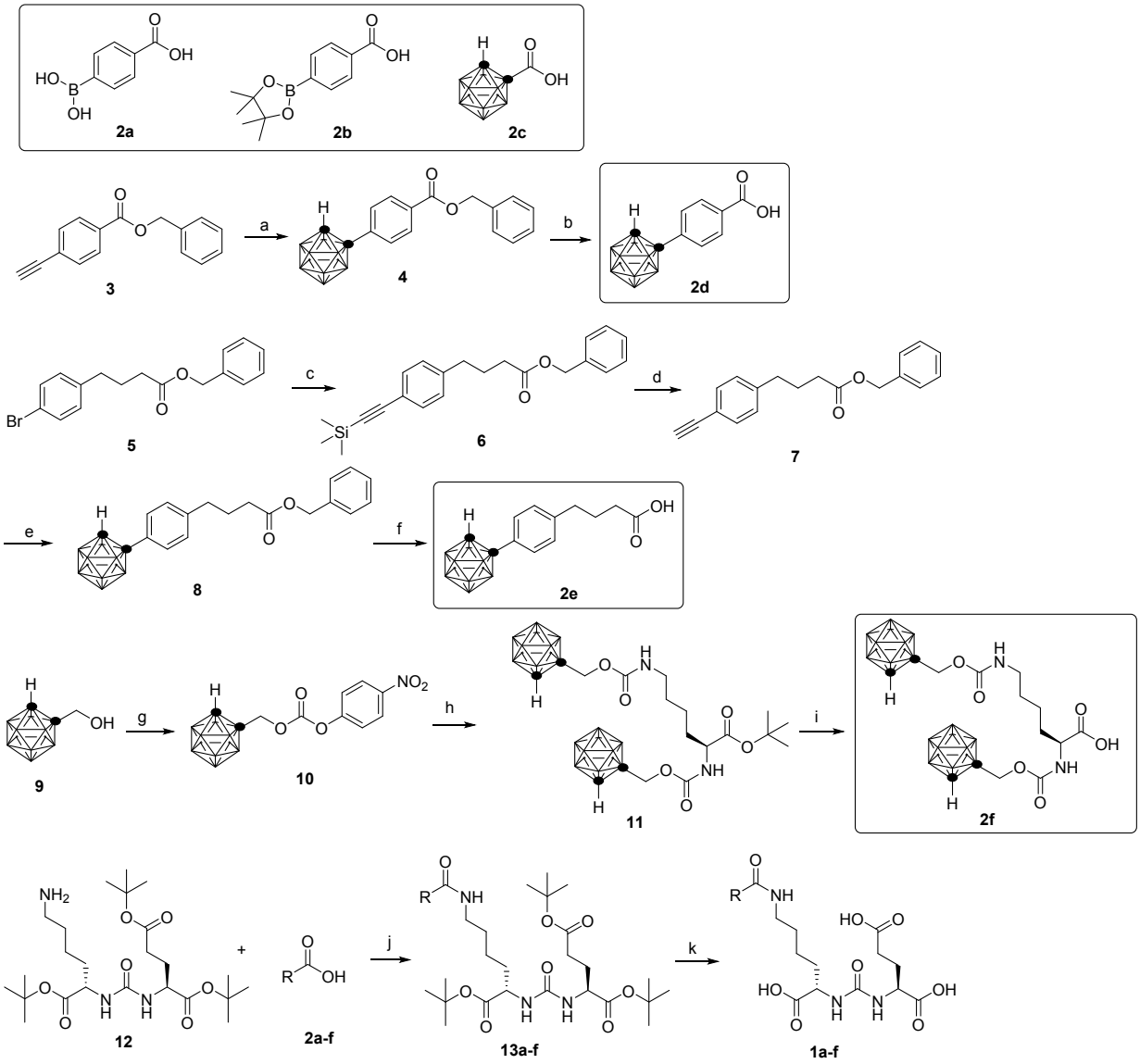

Scheme 1. Reagents and conditions for the synthesis of compounds 1a-f:

Key synthetic intermediates are outlined. (a) $B_{10}H_{12}(MeCN)_2$, $AgNO_3$, PhMe, 100 °C. (b) Pd/C, H_2, MeOH, rt. (c) trimethylsilyl acetylene, $PdCl_2(PPh_3)_2$, Et_3N, 70 °C. (d) Bu_4NF, THF, rt. (e)

$B_{10}H_{12}(MeCN)_2$, $AgNO_3$, PhMe, 100 °C. (f) Pd/C, H_2, MeOH, rt. (g) 4-nitrophenyl chloroformate, Et_3N, PhMe, 70 °C. (h) *L*-lysine *tert*-butyl ester, Et_3N, THF, rt. (i) TFA, DCM, rt. (j) DCC, NHS, THF, rt. (k) TFA, DCM.

3.2 Synthesis of Compounds 1g and 1h.

The synthesis of compound **1g** and **1h** is outlined in scheme 2. The starting material **15** was obtained following a known literature procedure.[33] Intermediate **10** was reacted with compound **12** or **15** followed by trifluoroacetic acid (TFA) deprotection to generate final compounds **1g** or **1h** respectively.

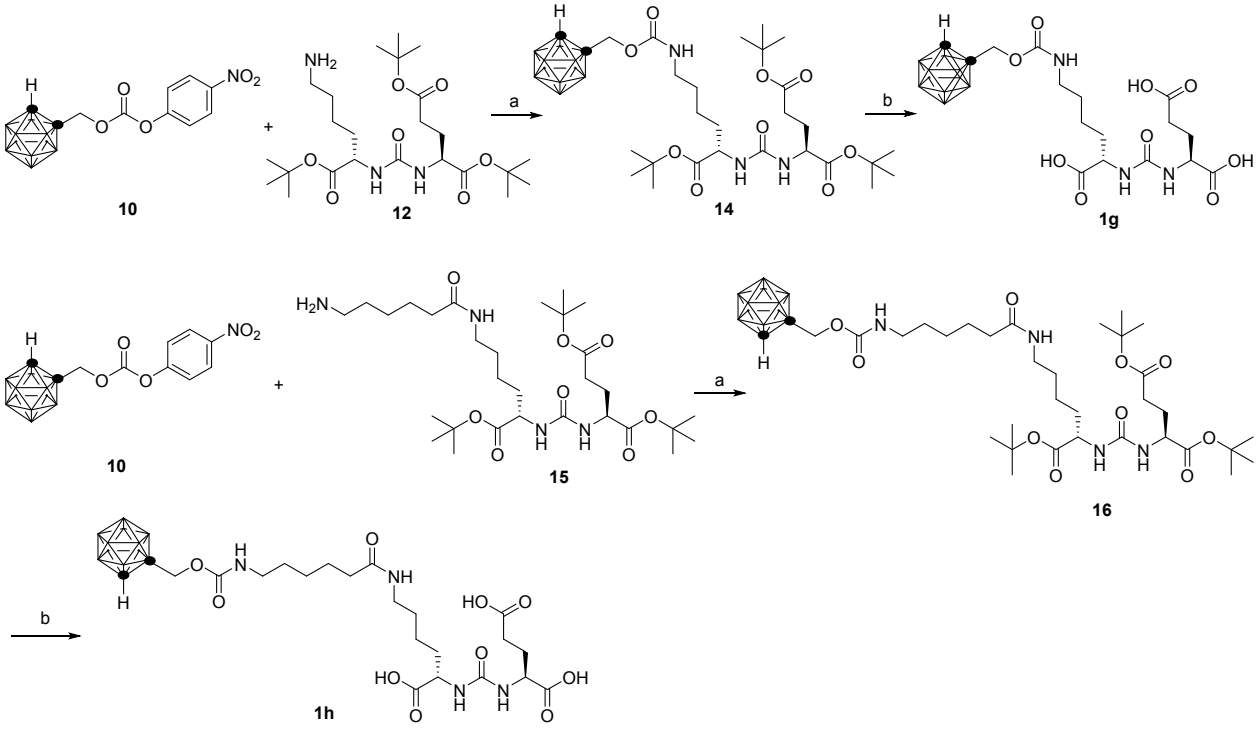

Scheme 2. Reagents and conditions for the synthesis of compounds 1g, 1h.

(a) Et_3N, THF, rt. (b) TFA, DCM, rt.

3.3 *In Vitro* Binding Studies

The relative binding affinities of compounds **1a-h** were determined using a ^{68}Ga-PSMA-11 competitive radioligand binding assay (Figure 2). The compounds that have been prepared are shown in Table 1. PMPA was selected for comparison and as a positive control.[27] In general, most of the compounds had a very high binding affinity, improved compared to PMPA, ranging

from approximately 20 – 550 nM. The relatively high IC_{50} for PMPA observed compared against a prior study may be due in part to the high affinity of the ^{68}Ga-PSMA-11 ligand used and/or differences in cell type.[25] Based on the IC_{50} values of compounds **1d**/**1e** and **1g**/**1h,** compounds with shorter linkers had higher binding affinities than compounds with longer linkers. The dicarborane compound **1f** had an increased $IC_{50,}$ possibly due to its branched structure and bulky size.

Based on these encouraging binding assays, three compounds were advanced for *in vivo* evaluation. Compound **1a** was selected for further study due to its good binding affinity, excellent water solubility and as a representative for the boronic acid PSMA inhibitor series, as a complement to the more hydrophobic carborane series. Carborane containing compound **1d** was selected since it showed the highest binding affinity. Compound **1f** was selected due to its highest boron content among the compounds (20 boron atoms per molecule).

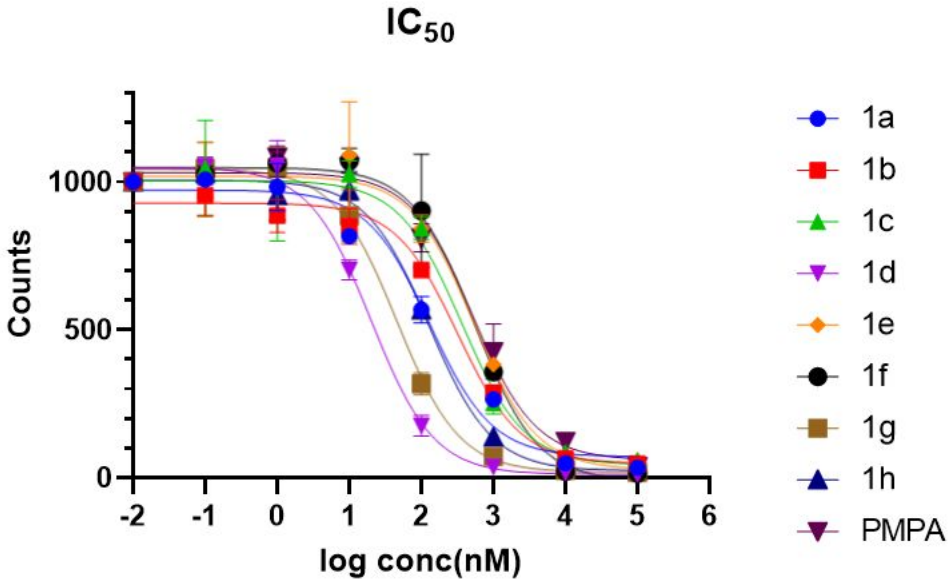

Figure 2. IC_{50} of compounds **1a-1h** determined by a competitive binding assay against ^{68}Ga-PSMA-11 on PSMA expressing 22Rv1 cells.

Table 1: IC_{50} of compounds **1a-1h** for PSMA$^{\alpha,\beta,\gamma}$.

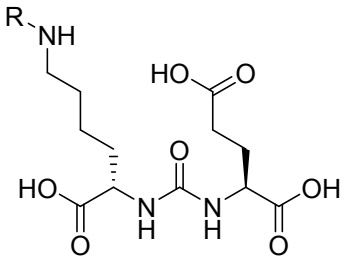

Entry	R	IC_{50} (nM)	Entry	R	IC_{50} (nM)
1a	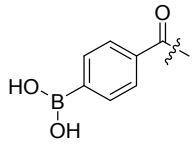	130.3±28.9	**1f**	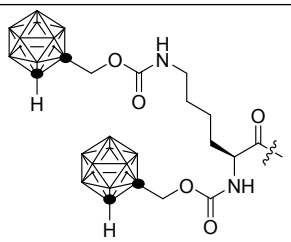	555.5±79.3
1b	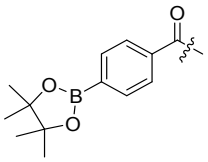	318.4±21.1	**1g**	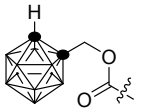	45.7±6.7
1c	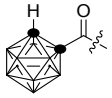	363.8±8.7	**1h**	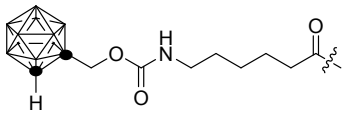	128.0±8.4
1d	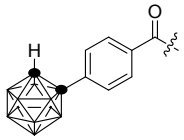	20.3±2.4	**control**	2-PMPA	523.5±84.0
1e	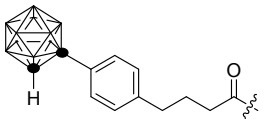	536.8±58.7			

[α] Cell line in all cases is 22Rv1. [β] The competitive binding compound is ^{68}Ga-PSMA-11. [γ] Cells were plated 48 h before testing (in triplicate). Various concentration (0.01-100000 nM) of compounds with 10 μCi of ^{68}Ga-PSMA-11 were added to cells and incubated for 1h. Cells were washed and lysed. A gamma counter was used to measure the bound fraction to the lysed cells.

3.4 LogP Hydrophobicity Assay, Internalization Assay and Serum Protein Binding Assay

The logP values of compound **1a**, **1d** and **1f** were measured to assess their hydrophilicity using the shake flask method and analysis of the resulting fractions via ICP-OES. Compared against the carborane containing compounds **1d** and **1f**, the boronic acid compound **1a** showed

increased hydrophilicity. A cellular internalization assay was performed in 22Rv1 cells. In the internalization assay, we found that a large portion of compound **1a** was bound at the membrane instead of being internalized into the cells. For compound **1d** and **1f**, most of the compounds were internalized into the cells (Table 2). The distribution of compounds **1a**, **1d** and **1f** in rat serum protein was measured. We found that only a small percentage of the tested compounds are bound to serum protein (supplemental table S2).

Table 2. Property of selected compounds

Compound	LogP	Internalization (x10^9 boron/cell)[α]	
		pellet	membrane
1a	−1.8 ± 0.2	0.14 ± 0.08	0.093 ± 0.053
1d	−0.2 ± 0.2	3.3 ± 0.62	0.22 ± 0.04
1f	0.2 ± 0.2	4.2 ± 1.9	0.14 ± 0.063

[α] 100 μM selected compounds were incubated with cells for 1 h.

3.5 Cell Toxicity Assay and Acute Toxicity Assays

Compounds **1a**, **1d** and **1f** were selected for cell toxicity assay using the CellTiter-Glo assay. After incubating 22Rv1 with these three tested compounds for 4 hours, no obvious toxicity was observed for all of the three compounds even up to 100 μM, suggesting a low cell toxicity of these compounds (supplemental table S3 and figure S1).

A preliminary acute toxicity assay was performed prior to biodistribution and imaging studies. Compound **1a** was dissolved in 200 μL of PBS. Compound **1d** or **1f** was dissolved in a mixture of 40 μL of DMSO and 160 μL of PBS. Non-tumor bearing male athymic mice were administered graded doses of the selected boronated compounds via intraperitoneal injection (5 mg/mouse, 7.5 mg/mouse, 15 mg/mouse or 30mg/mouse), and were monitored closely. Compound **1a** demonstrated no acute toxicity up to 30 mg per mouse. For compound **1d** and **1f**, the maximum tolerated dose was 5 mg per mouse and 7.5 mg per mouse, respectively. When 7.5 mg **1d**/mouse or 15 mg **1f**/mouse was administered, one mouse in each group demonstrated acute toxicity requiring euthanasia (supplemental table S4). No obvious hemorrhages or damaged organs were observed on gross dissection.

3.6 Outline of *In Vivo* PET Imaging and Biodistribution Assays

Next, we determined the ability of the boron labeled PSMA agents to bind to PSMA *in vivo* using a PET imaging assay, and determined the boron biodistribution by harvesting the organs

and recording ICP-OES of the resulting tissues (Figure 3). The *in vivo* ^{68}Ga-PSMA-11 blocking assay and boron biodistribution studies were performed in athymic mice bearing 22Rv1 tumor xenografts three weeks post inoculation. The study population consisted of nine groups (n = 4 mice for each group). Vehicle (PBS) was used as a negative control. Boronophenylalanine (BPA) is the most widely used compound in BNCT clinical trials, and was included for comparison.[34] Tested compounds were administered followed by the injection of approximately 100 μCi (3.7 MBq) of ^{68}Ga-PSMA-11. For the vehicle group, mice were imaged after 1 hour post injection and were immediately sacrificed for organ collection after imaging. For each of BPA and candidate compounds **1a**, **1d** and **1f**, mice were split to either the 1 hour group or the 4 hour group. For the 1 hour group, mice were sacrificed and their organs were collected at 1 hour post injection. For the 4 hour group, mice were imaged at 1 hour post injection and were subsequently sacrificed at 4 hour post injection for organ collection.

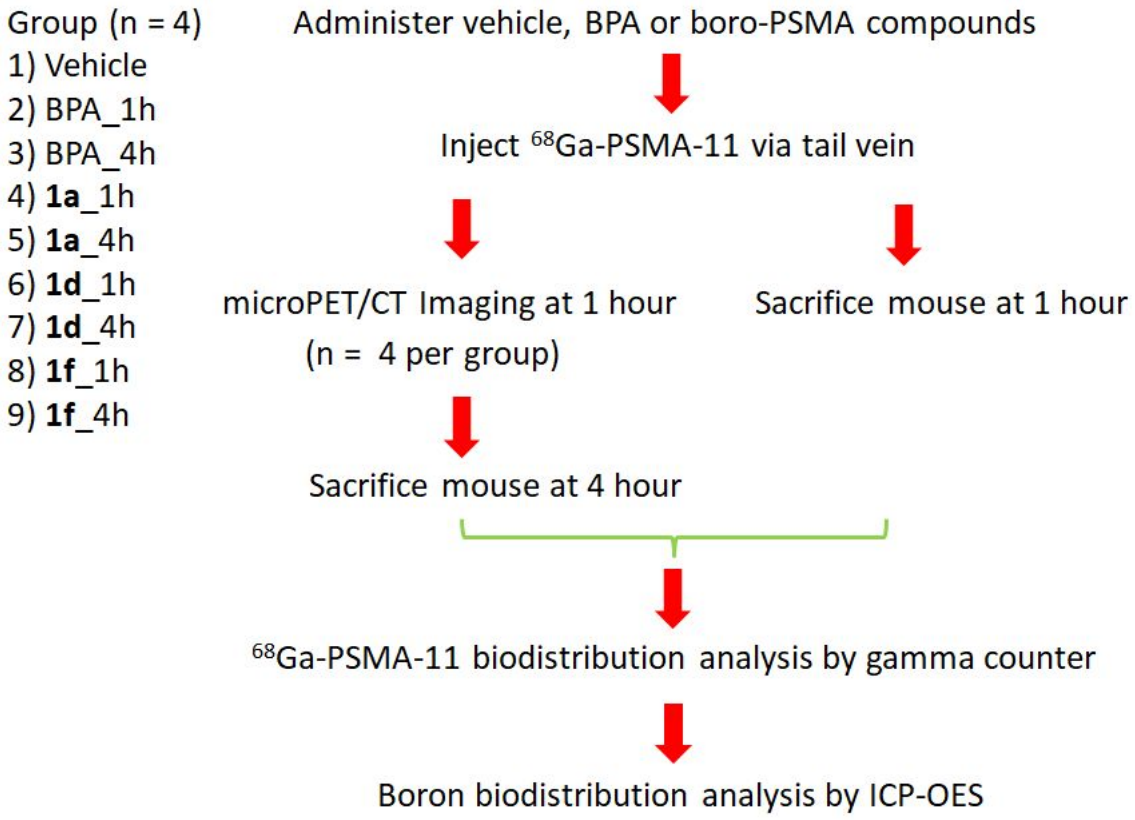

Figure 3. Flow chart of PET imaging, ^{68}Ga-PSMA-11 biodistribution and boron biodistribution assay performed in mice bearing 22Rv1 xenograft tumors.

3.7 *In Vivo* PET Imaging and ^{68}Ga-PSMA-11 Biodistribution Analysis

Analysis of the micro PET/CT images demonstrated that for the vehicle and BPA group, there was high ^{68}Ga-PSMA-11 uptake in the tumor, as expected based on the known expression of PSMA in 22Rv1 xenografts.[35,36] On the other hand, boron-containing PSMA inhibitors **1a**, **1d**, and **1f** blocked ^{68}Ga-PSMA-11 uptake in the tumors, demonstrating the strong *in vivo* binding between boron-containing PSMA inhibitors and PSMA (Figure 4A). The ^{68}Ga-PSMA-11 biodistribution showed high uptake in kidney, spleen and tumor, similar with previously published results.[36] As expected, the addition of BPA did not significantly block uptake in target organs including kidney, spleen and tumor. Unexpectedly, there was an apparent increase in the blood and tumor concentration of ^{68}Ga-PSMA-11 with BPA treatment. The reasons for this are unclear, but may relate to changes in metabolism and/or clearance pathways induced by BPA treatment. In contrast, **1a** and **1d** significantly reduced the uptake of ^{68}Ga-PSMA-11 in kidney, spleen and tumor. Compound **1f** reduced uptake of ^{68}Ga-PSMA-11 in spleen and tumor, but there was still moderate amount of uptake at kidney (Figure 4B). The tumor/blood ratio and tumor/muscle ratio showed a decrease when inhibitors were administered (Figure 4C). For compound **1a** and **1d**, the ratio markedly increased after 4 hour compared to 1 hour, while for compound **1f**, the ratio only slightly increased, which indicates a longer circulation life time of **1f**. Similar results were obtained through region of interest analysis of the micro PET/CT images (supplemental table S5 and S6). Taken together, these data indicate that boron labeled PSMA inhibitors **1a**, **1d**, and **1f** are able to block ^{68}Ga-PSMA-11 uptake in target tissues including tumor and kidney, suggesting a high degree of receptor occupancy *in vivo*.

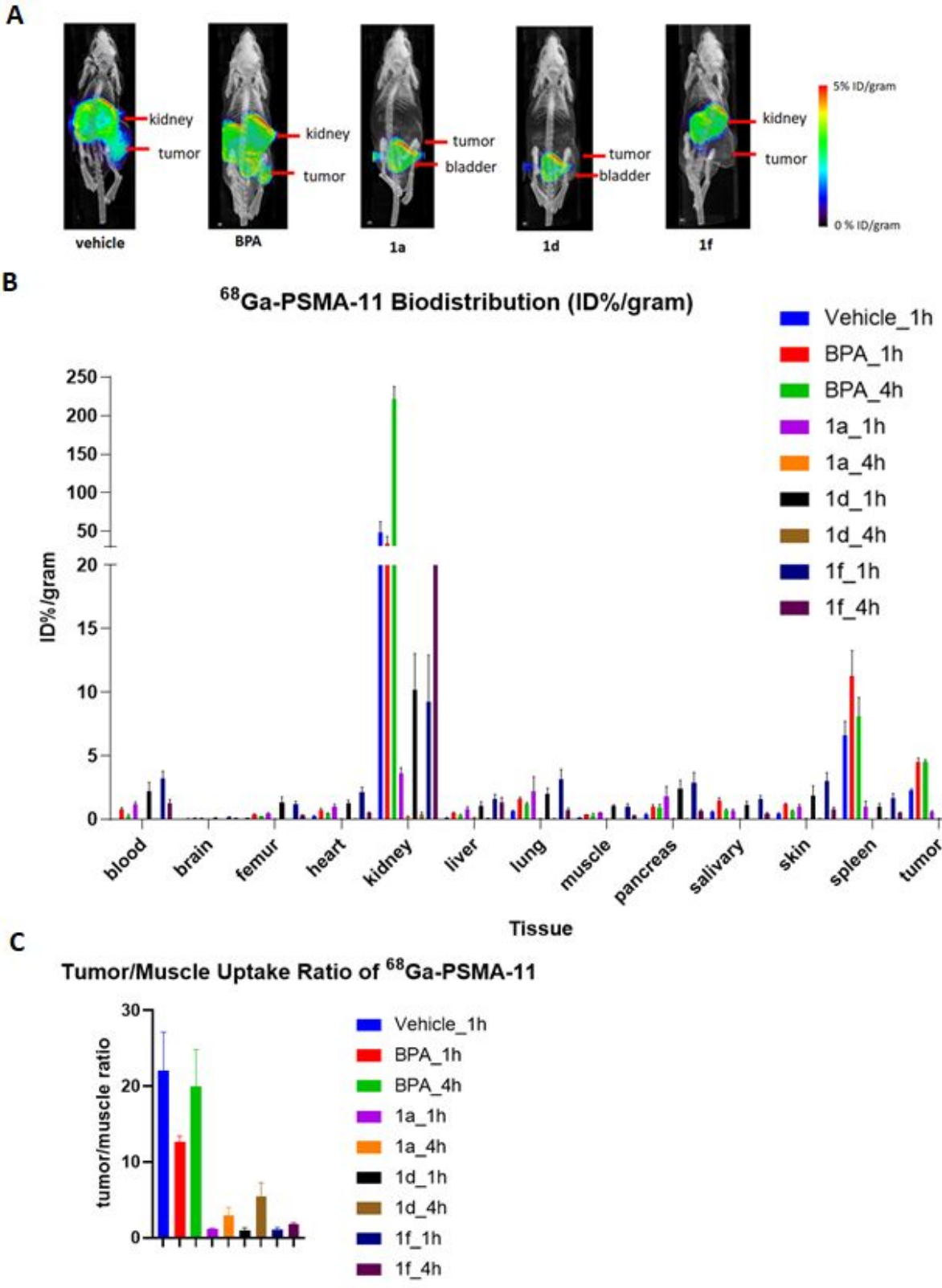
A
kidney
tumor
vehicle
kidney
tumor
BPA
tumor
bladder
1a
tumor
bladder
1d
kidney
tumor
1f
5% ID/gram
0 % ID/gram
B
68Ga-PSMA-11 Biodistribution (ID%/gram)
Vehicle_1h
BPA_1h
BPA_4h
1a_1h
1a_4h
1d_1h
1d_4h
1f_1h
1f_4h
ID%/gram
250
200
150
100
50
20
15
10
5
0
blood
brain
femur
heart
kidney
liver
lung
muscle
pancreas
salivary
skin
spleen
tumor
Tissue
C
Tumor/Muscle Uptake Ratio of 68Ga-PSMA-11
tumor/muscle ratio
30
20
10
0
Vehicle_1h
BPA_1h
BPA_4h
1a_1h
1a_4h
1d_1h
1d_4h
1f_1h
1f_4h

Figure 4. (A) PET imaging results showed efficient blocking of ^{68}Ga-PSMA-11 uptake by boro-PSMA compounds, but not by BPA. (B) ^{68}Ga-PSMA-11 biodistribution as determined by collection of organs and gamma counting. (C) Tumor/muscle uptake ratio of ^{68}Ga-PSMA-11.

3.8 *In Vivo* Boron Biodistribution Analysis

The organs collected were also subjected to ICP-OES to assay total boron content (Figure 5A and Figure S2 in Supplementary). As expected, the vehicle group resulted in minimal boron uptake in tissue when no boron compounds were administered. The known BNCT compound BPA demonstrated accumulation at blood, kidney, pancreas and especially liver. For **1a**, the blood boron content significantly decreased at 4 hour compared to 1 hour from 7.8 μg/gram tissue to 1.7 μg/gram, suggesting quick clearance of this compound. There was more uptake in kidney than in liver, suggesting primarily renal elimination, as expected based on its hydrophilic character. The tumor boron uptake was 4.1 μg/gram tissue, which is similar to boron uptake in muscle (3.8 μg/gram). For compound **1d**, the blood boron content slightly decreased at 4 hour compared to 1 hour from 22.5 μg/gram tissue to 17.1 μg/gram tissue, indicating a longer circulation time *in vivo*. More uptake was observed in liver than in kidney, suggesting primarily hepatobiliary clearance. The boron uptake in tumor was 4.4 μg/gram tissue at 1 hour, similar to the boron uptake in muscle (4.4 μg/gram). However, the boron uptake in tumor was 4.2 μg/gram tissue at 4 hour, two fold higher than the boron uptake in muscle (2.2 μg/gram tissue) (Figure 5C). For compound **1f**, the blood boron content significantly increased at 4 hour compared to 1 hour from 17.4 μg/gram tissue to 78.3 μg/gram tissue, suggesting a slow absorption and long circulation time for the compound in mice. The liver had greater uptake than kidney, again suggesting hepatobiliary clearance. The tumor boron uptake is 3.3 μg/gram tissue at 1 hour and 3.4 μg/gram tissue at 4 hour, which was lower than the boron uptake in muscle (5.1 μg/gram tissue and 5.1 μg/gram tissue, respectively). Overall, the more hydrophobic compounds **1d** and **1f** had a longer circulation time in blood. Similar total tumor uptake, ranging from 3.3 – 7.1 μg/gram was seen between BPA, compounds **1d**, and **1f,** while compound **1a** demonstrated decreased tumor uptake at four hours.

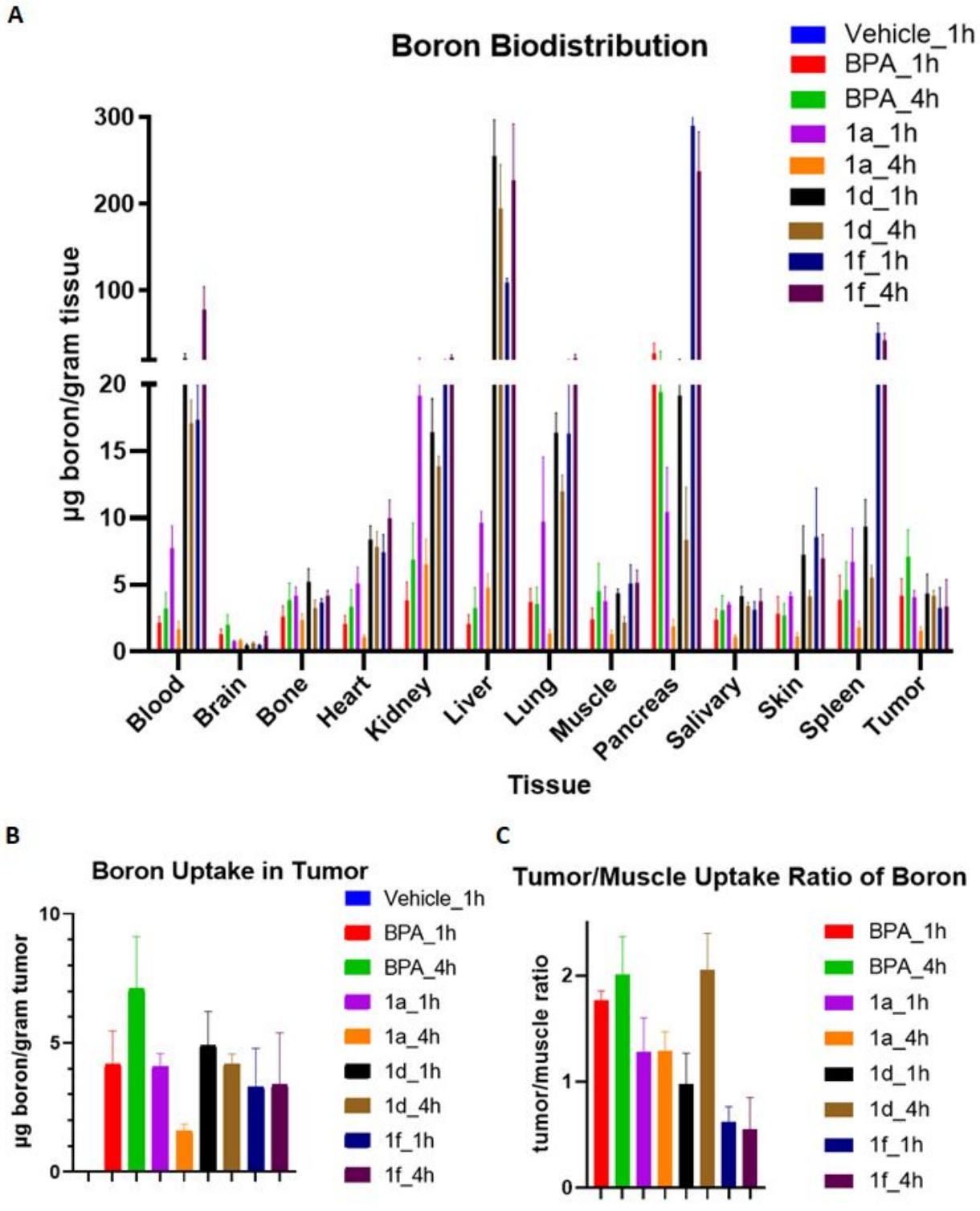
A
Boron Biodistribution
Vehicle_1h
BPA_1h
BPA_4h
1a_1h
1a_4h
1d_1h
1d_4h
1f_1h
1f_4h
µg boron/gram tissue
300
200
100
20
15
10
5
0
Blood
Brain
Bone
Heart
Kidney
Liver
Lung
Muscle
Pancreas
Salivary
Skin
Spleen
Tumor
Tissue
B
Boron Uptake in Tumor
µg boron/gram tumor
10
5
0
C
Tumor/Muscle Uptake Ratio of Boron
tumor/muscle ratio
2
1
0

D

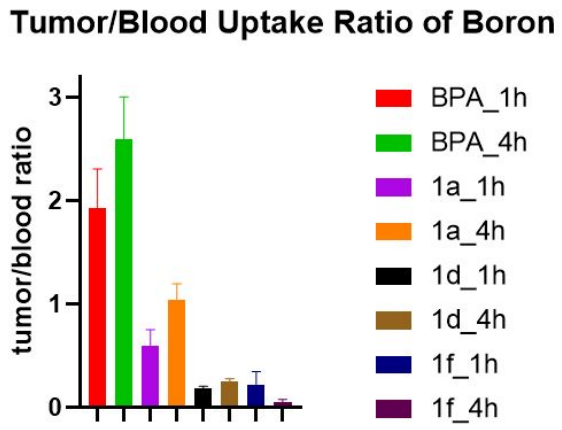

Figure 5. (A) Boron biodistribution. Tissues were harvested as indicated in figure 3, homogenized and boron content was determined by ICP-OES. (B) Boron uptake in tumor (C) Tumor/muscle uptake ratio of boron. (D) Tumor/blood uptake ratio of boron.

■ DISCUSSION

In this report, we demonstrate the synthesis and initial *in vitro* and *in vivo* evaluation of a series of boron-containing PSMA inhibitors based around a common urea skeleton. Although all these eight Boro-PSMA compounds share the same urea-based PSMA binding skeleton, the alteration of the side chain significantly influenced their binding affinity, cell internalization ability and pharmacokinetics. Overall, all compounds demonstrated equal to or improved ability to bind PSMA based on a competition radioligand binding assay, when compared against known high affinity PSMA inhibitor, PMPA. The very high binding affinity of these compounds is not surprising given the well-known versatility of the urea-based PSMA binding scaffold.[37,38,39]

Based on these encouraging initial results, three compounds were advanced to initial *in vivo* testing using imaging and boron biodistribution assays. Compound **1a** was selected as a hydrophilic, single boron containing agent. Compound **1d** was selected as a representative of the carborane group, with the highest overall IC_{50} of 20.3 nM. Compound **1f** was selected as it had two carborane substituents and the largest number of boron atoms (20) as well as reasonable binding affinity. All three compounds demonstrated high PSMA binding *in vivo* as demonstrated by PET imaging and ^{68}Ga-PSMA-11 biodistribution analysis, while BPA did not demonstrate *in vivo* PSMA binding. However, the boro-PSMA compounds demonstrated differing

pharmacokinetics and overall tumor boron uptake. The hydrophilic compound **1a** demonstrated rapid renal clearance, and efficient binding of PSMA *in vivo* as judged by the blocking of ^{68}Ga-PSMA-11 uptake in tumor. However, the overall tumor boron uptake was the lowest of all compounds tested at four hours, despite the highest administered dose, possibly due to only a single boron atom per molecule. Overall, compound **1a** is a very hydrophilic molecule due to its three carboxylic acids and the boronic acid group. In contrast, the more hydrophobic carborane compounds **1d** and **1f** demonstrated primary hepatobiliary clearance, while still demonstrating efficient ^{68}Ga-PSMA-11 blocking *in vivo*. The *in vivo* half life of these compounds appeared to be significantly greater than **1a** as judged by the high residual boron content in the blood at four hours after administration. Compounds **1d** and **1f** demonstrated similar overall boron uptake in tumor when compared against BPA, the most commonly used agent for BNCT. However, an unexpected result is that the increased boron content per molecule did not increase the uptake of **1f** in tumor when compared against **1d**, possibly because of slow absorption. For compound **1d** and **1f**, the boron concentration in the blood was still high after 4 hours, indicating an increased boron uptake at tumor after 4 hours, but also a higher risk of toxicity.

In this study, we assayed the receptor engagement through competition binding assays with ^{68}Ga-PSMA-11 PET, and direct tumoral uptake through biodstribution assays and ICP-MS of total tissue boron content. Another alternative way to determine biodistribution of boron containing compounds could be considered for future studies using direct labeling of the Boro-PSMA derivatives with chelators (DOTA, DTPA), that can coordinate metal imaging probes such as ^{68}Ga for PET or Gd for MRI.[40,41]

To date, there have been two reports of boro-PSMA inhibitors. Byun's group reported the synthesis of carborane containing PSMA inhibitors and a PSMA-inhibitor X-ray structural characterization.[24] However, the compounds were not further evaluated in animal models. Valliant's group also produced a series of carborane containing PSMA inhibitors, but the IC_{50} were not improved compared to PMPA.[25] In contrast, the boro-PSMA inhibitors in our study exhibited a significantly enhanced IC_{50} up to 26-fold reduced compared to PMPA. We also further revealed their structure activity relationship, proved their *in vivo* binding of PSMA, determined their boron biodistribution and tumor uptake in a 22Rv1 xenograft mice model. Taken together, these experiments demonstrate similar overall uptake of Boro-PSMA compounds **1d** and **1f** when compared against BPA, the most commonly used BNCT agent.

When compared against the previously reported studies evaluating BPA uptake in tumor, our BPA results demonstrate a tumor/muscle uptake ratio of 2.0 at 4 hour time point, consistent with other prior reports ranging between 1.5 and 4.4.[42] In our study, the BPA uptake at tumor is 7.1±4.0 μg/gram at 4 hour. Overall, the BPA biodistribution results are similar to prior reports conducted under similar conditions.[43,44]

A tumor uptake of at least 20-50 μg/gram boron is typically thought to be necessary for effective tumor therapy. The boron ratio in tumor/normal tissue needs to be greater than 3:1 for selectivity.[3] However, the boron uptake did not reach the requirements, suggesting that the current compounds and/or dosing regimens are not sufficient for therapy. In order to deliver sufficient boron to the tumor, both high affinity binding and high abundance targets are required. In this study, a large amount of boron compound was administered, saturating PSMA binding sites *in vivo* as verified using the ^{68}Ga-PSMA-11 binding and blocking assay. Several approaches could be used to improve boron delivery to tumor. Firstly, the timing and route of administration of the compounds could be varied. The very high blood content of compounds **1d** and **1f** at the latest time point tested, as well as the increased tumor to muscle ratio at four hours compared against one hour, suggests that a longer incubation time could improve the overall boron delivery as well as tumor to blood and tumor to muscle ratios. The second potential route for improvement would be to include larger numbers of boron atoms per PSMA-inhibitor. While compound **1f** contains 20 atoms, larger substitutents such as dendrimers and nanoparticles have been reported.[45,46,47,48,49] In principle, these substituents could be appended to the urea-based PSMA agent to achieve higher boron delivery. Finally, the use of animal models with increased PSMA expression would likely yield improved tumor boron uptake. While the 22Rv1 model was selected due to convenient, rapid and predictable tumor growth, its overall PSMA expression is low compared against other cell lines such as LNCaP or PC3-pip.[50] These improvements to the method represent important areas for future investigation. Following optimization of the pharmacokinetics, and dosing regimens, initial treatment studies could be performed in mice bearing appropriate tumor xenografts.

■ CONCLUSION

In this study, a series of boronic acid- and carborane-containing PSMA inhibitors were successfully synthesized. The *in vitro* binding data demonstrated high binding affinities to

PSMA for all the boron-containing inhibitors. In particular, compound **1d** showed a 26 fold lower IC_{50} value that the well-known PSMA inhibitor PMPA. PET imaging data demonstrated blocking of ^{68}Ga-PSMA-11 uptake by boron containing PSMA compounds, demonstrating the *in vivo* binding of the PSMA inhibitors to their target. The boron uptake and distribution assay showed around 4 μg boron/gram tumor uptake and similar tumor/muscle ratios compared to the ratio for the standard compound BPA. Although the uptake is below the required 20 μg boron/gram tumor threshold, these data suggest that with further optimization, treatment of oligometastatic prostate cancer with Boro-PSMA is feasible.

■ ABBREVIATIONS

BNCT: boron neutron capture therapy; PSMA: prostate specific membrane antigen; PET: positron emission tomography; LET: linear energy transfer; BPA: 4-borono-*L*-phenylalanine; BSH: sodium borocaptate; PCa: prostate cancer; GCPII: glutamate carboxypeptidase II; FBS: fetal bovine serum; PMPA: 2-(phosphonomethyl) pentanedioic acid; ICP-OES: inductively coupled plasma optical-emission spectrometry. IACUC: Institutional Animal Care & Use Program; DCC: *N,N*′-Dicyclohexylcarbodiimide; NHS: *N*-Hydroxysuccinimide; TFA: trifluoroacetic acid.

■ ASSOCIATED CONTENT

Supporting Information

The Supporting Information is available free of charge on the ACS Publications website at DOI: Synthesis procedure, ^{1}H and ^{13}C NMR spectra of compounds **1a-h**, supplementary figures and tables.

■ AUTHOR INFORMATION

Corresponding Author

*Robert Flavell, Tel: +1-415-3533638; E-mail: robert.flavell@ucsf.edu.

Notes

The authors have declared that no competing interest exists

■ ACKNOWLEDGMENTS

This work was supported by an American Cancer Society Individual Research Grant (IRG-97-150-13), and the New Directions in Prostate Cancer Research Award of the University of California, San Francisco Prostate Cancer Research Program. This publication was supported by the Helen Diller Family Comprehensive Cancer Center Support Grant of the National institutes of Health under P30 CA 82103. Dr. Flavell was additionally supported by the David Blitzer Young Investigator Award of the Prostate Cancer Foundation and a Physician Research Training Grant from the Department of Defense (PC 150932). We thank Dr. Rob Franks and Dr. Brian Dreyer of the Marine Analytical Laboratory in the University of California, Santa Cruz for assistance with ICP measurements, Kyoughee Seo in the University of California, San Francisco for help with mice dissection.

■ REFERENCES

(1) Heber, E. M.; Hawthorne, M. F.; Kueffer, P. J.; Garabalino, M. A.; Thorp, S. I.; Pozzi, E. C. C.; Hughes, A. M.; Maitz, C. A.; Jalisatgi, S. S.; Nigg, D. W.; Curotto, P., Trivillin V. A.; Schwint, A. E. Therapeutic efficacy of boron neutron capture therapy mediated by boron-rich liposomes for oral cancer in the hamster cheek pouch model. *Proc. Natl. Acad. Sci.* **2014**, *111*, 16077-16081.

(2) Nedunchezhian, K.; Aswath, N.; Thiruppathy, M.; Thirugnanamurthy, S. Boron neutron capture therapy - a literature review. *J. Clin. Diagnostic Res.* **2016**, *10*, ZE01-ZE04.

(3) Barth, R. F.; Mi, P.; Yang, W. Boron delivery agents for neutron capture therapy of cancer. Cancer Commun. **2018**, *38*, 1–15.

(4) Pozzi, E. C. C.; Cardoso, J. E.; Colombo, L. L.; Thorp, S.; Hughes, A. M.; Molinari, A. J.; Garabalino, M. A.; Heber, E. M.; Miller, M.; Itoiz, M. E.; Aromando, R. F.; Nigg, D. W.; Quintana, J.; Trivillin, V. A. Schwint, A. E. Boron neutron capture therapy (BNCT) for liver metastasis: therapeutic efficacy in an experimental model. *Radiat. Environ. Biophys.* **2012**, *51*, 331–339.

(5) Haapaniemi, A.; Kankaanranta, L.; Saat, R.; Koivunoro, H.; Saarilahti, K.; Mäkitie, A.; Atula, T.; Joensuu, H. Boron neutron capture therapy in the treatment of recurrent laryngeal cancer. *Int. J. Radiat. Oncol. Biol. Phys.* **2016**, *95*, 404–410.

(6) Chanana, A. D.; Capala, J.; Chadha, M.; Coderre, J. A.; Diaz, A. Z.; Elowitz, E. H.; Iwai, J.; Joel, D. D.; Liu, H. B.; Ma, R.; Pendzick, N.; Peress, N. S.; Shady, M. S.; Slatkin, D.N.; Tyson, G.W.; Wielopolski, L. Boron neutron capture therapy for glioblastoma multiforme: interim results from the phase I/II dose-escalation studies. *Neurosurgery* **1999**, *44,* 1182–1193.

(7) Barth, R. F.; Coderre, J. A.; Vicente, M. G. H.; Blue, T. E. Boron neutron capture therapy of cancer: current status and future prospects. *Clinical Cancer Research*. **2005**, *11*, 3987–4002.

(8) Barth, R. F.; Vicente, M. G. H.; Harling, O. K.; Kiger, W. S.; Riley, K. J.; Binns, P. J.; Wagner, F. M.; Suzuki, M.; Aihara, T.; Kato, I.; Kawabata, S. Current status of boron neutron capture therapy of high grade gliomas and recurrent head and neck cancer. *Radiation Oncology*. **2012**, *7*, 1–21.

(9) Henriksson, R.; Capala, J.; Michanek, A.; Lindahl, S. Å.; Salford, L. G.; Franzén, L.;

Blomquist, E.; Westlin, J. E.; Bergenheim, A. T. Boron neutron capture therapy (BNCT) for glioblastoma multiforme: a phase II study evaluating a prolonged high-dose of boronophenylalanine (BPA). *Radiother. Oncol.* **2008**, *88*, 183-191.
(10) Takagaki, M.; Oda, Y.; Miyatake, S. I.; Kikuchi, H.; Kobayashi, T.; Sakurai, Y.; Osawa, M.; Mori, K.; Ono, K. Boron neutron capture therapy: preliminary study of BNCT with sodium borocaptate ($Na_2B_{12}H_{11}SH$) on glioblastoma. *J. Neurooncol.* **1997**, *35*, 177-185.
(11) Haritz, D.; Gabel, D.; Huiskamp, R. Clinical phase-I study of $Na_2B_{12}H_{11}SH$ (BSH) in patients with malignant glioma as precondition for boron neutron capture therapy (BNCT). *Int. J. Radiat. Oncol. Biol. Phys.* **1994**, *28*, 1175-1181.
(12) Johansson, J. E.; Andrén, O.; Andersson, S. O.; Dickman, P. W.; Holmberg, L.; Magnuson, A.; Adami, H. O. Natural history of early, localized prostate cancer. *J. Am. Med. Assoc.* **2004**, *291*, 2713-2719.
(13) Bray, F.; Ferlay, J.; Soerjomataram, I.; Siegel, R. L.; Torre, L. A.; Jemal, A. Global cancer statistics 2018: GLOBOCAN estimates of incidence and mortality worldwide for 36 cancers in 185 countries. *CA. Cancer J. Clin.* **2018**, *68*, 394–424.
(14) Perner, S.; Hofer, M. D.; Kim, R.; Shah, R. B.; Li, H.; Möller, P.; Hautmann, R. E.; Gschwend, J. E.; Kuefer, R.; Rubin, M. A. Prostate-specific membrane antigen expression as a predictor of prostate cancer progression. *Hum. Pathol.* **2007,** *38*, 696-701.
(15) Maurer, T.; Eiber, M.; Schwaiger, M.; Gschwend, J. E. Current use of PSMA-PET in prostate cancer management. *Nature Reviews* **2016**, *13*, 226-235.
(16) Eder, M.; Schäfer, M.; Bauder-Wüst, U.; Hull, W. E.; Wängler, C.; Mier, W.; Haberkorn, U.; Eisenhut, M. ^{68}Ga-Complex lipophilicity and the targeting property of a urea-based PSMA inhibitor for PET imaging. *Bioconjug. Chem.* **2012**, *23*, 688-697.
(17) Hillier, S. M.; Maresca, K. P.; Femia, F. J.; Marquis, J. C.; Foss, C. A.; Nguyen, N.; Zimmerman, C. N.; Barrett, J. A.; Eckelman, W. C.; Pomper, M. G.; Joyal, J. L.; Babich, J. W. Preclinical evaluation of novel glutamate-urea-lysine analogues that target prostate-specific membrane antigen as molecular imaging pharmaceuticals for prostate cancer. *Cancer Res.* **2009**, *69*, 6932-6940.
(18) Barinka, C.; Byun, Y.; Dusich, C. L.; Banerjee, S. R.; Chen, Y.; Castanares, M.; Kozikowski, A. P.; Mease, R. C.; Pomper, M. G.; Lubkowski, J. Interactions between Human Glutamate Carboxypeptidase II and Urea-Based Inhibitors: Structural Characterization. *J. Med. Chem.* **2008**, *51*, 7737-7743.
(19) Fendler, W. P.; Rahbar, K.; Herrmann, K.; Kratochwil, C.; Eiber, M. ^{177}Lu-PSMA radioligand therapy for prostate cancer. *J. Nucl. Med.* **2017**, *58*, 1196-1200.
(20) Kratochwil, C.; Bruchertseifer, F.; Giesel, F. L.; Weis, M.; Verburg, F. A.; Mottaghy, F.; Kopka, K.; Apostolidis, C.; Haberkorn, U.; Morgenstern, A. ^{225}Ac-PSMA-617 for PSMA-targeted radiation therapy of metastatic castration-resistant prostate cancer. *J. Nucl. Med.* **2016**, *57*, 1941-1944.
(21) Hrkach, J.; Von Hoff, D.; Ali, M. M.; Andrianova, E.; Auer, J.; Campbell, T.; De Witt, D.; Figa, M.; Figueiredo, M.; Horhota, A.; Low, Susan; McDonnell, K.; Peeke, E.; Retnarajan, B.; Sabnis, A.; Schnipper, E.; Song, J. J.; Song, Y. H.; Summa, J.; Tompsett, D.; Troiano, G.; Van Geen Hoven, T.; Wright, J.; LoRusso, P.; Kantoff, P. W.; Bander, N. H.; Sweeney, C.; Farokhzad, O. C.; Langer, R.; Zale, S. Preclinical development and clinical translation of a PSMA-targeted Docetaxel nanoparticle with a differentiated pharmacological profile. *Sci. Transl. Med.* **2012**, *4*, 128-139.
(22) Wang, X.; Ma, D.; Olson, W. C.; Heston, W. D. W. *In Vitro* and *In Vivo* Responses of

advanced prostate tumors to PSMA ADC, an Auristatin-conjugated antibody to prostate-specific membrane antigen. *Mol. Cancer Ther.* **2011**, *10*, 1728-1739.
(23) Xiang, B.; Dong, D. W.; Shi, N. Q.; Gao, W.; Yang, Z. Z.; Cui, Y.; Cao, D. Y.; Qi, X. R. PSA-responsive and PSMA-mediated multifunctional liposomes for targeted therapy of prostate cancer. *Biomaterials* **2013**, *34*, 6976-6991.
(24) Youn, S.; Kim, K. I.; Ptacek, J.; Ok, K.; Novakova, Z.; Kim, Y. H.; Koo, J. H.; Barinka, C.; Byun, Y. Carborane-containing urea-based inhibitors of glutamate carboxypeptidase II: synthesis and structural characterization. *Bioorganic Med. Chem. Lett.* **2015**, *25*, 5232–5236.
(25) El-Zaria, M. E.; Genady, A. R.; Janzen, N.; Petlura, C. I.; Beckford Vera, D. R.; Valliant, J. F. Preparation and evaluation of carborane-derived inhibitors of prostate specific membrane antigen (PSMA). *Dalt. Trans.* **2014**, *43*, 4950–4961.
(26) Nanabala, R.; Anees, M. K.; Sasikumar, A.; Joy, A.; Pillai, M. R. A. Preparation of [^{68}Ga]PSMA-11 for PET-CT imaging using a manual synthesis module and organic matrix based ^{68}Ge/^{68}Ga generator. *Nucl. Med. Biol.* **2016**, *43*, 463–469.
(27) Mesters, J. R.; Henning, K.; Hilgenfeld, R. Human glutamate carboxypeptidase II inhibition: structures of GCPII in complex with two potent inhibitors, Quisqualate and 2-PMPA. *Acta Crystallogr. Sect. D Biol. Crystallogr.* **2007,** *63*, 508-513.
(28) Leo, A.; Hansch, C.; Elkins, D. Partition coefficients and their uses. *Chem. Rev.* **1971**, *71*, 525–616.
(29) García, L. A.; Arias, E.; Moggio, I.; Romero, J.; Ledezma, A.; Ponce, A.; Perez, O. Fluorescent core-sheath fibers by electrospinning of a phenyleneethynylene/ poly(styrene-co-maleimide) blend. *Polymer* **2011**, *52*, 5326–5334.
(30) Wakasugi, K.; Iida, A.; Misaki, T.; Nishii, Y.; Tanabe, Y. Simple, mild, and practical esterification, thioesterification, and amide Formation utilizing p-toluenesulfonyl chloride and *N*-methylimidazole. *Adv. Synth. Catal.* **2003**, *345*, 1209-1214.
(31) Toppino, A.; Genady, A. R.; El-Zaria, M. E.; Reeve, J.; Mostofian, F.; Kent, J.; Valliant, J. F. High yielding preparation of dicarba-closo-dodecaboranes using a silver(I) mediated dehydrogenative alkyne-insertion reaction. *Inorg. Chem.* **2013**, *52*, 8743–8749.
(32) Wang, M.; McNitt, C. D.; Wang, H.; Ma, X.; Scarry, S. M.; Wu, Z.; Popik, V. V.; Li, Z. The efficiency of ^{18}F labelling of a prostate specific membrane antigen ligand via strain-promoted azide-alkyne reaction: reaction speed versus hydrophilicity. *Chem. Commun.* **2018**, *54*, 7810-7813.
(33) Cleeren, F.; Lecina, J.; Billaud, E. M. F.; Ahamed, M.; Verbruggen, A.; Bormans, G. M. New chelators for low temperature Al^{18}F-labeling of biomolecules. *Bioconjug. Chem.* **2016**. *27*, 790-798.
(34) Capala, J.; Britta, H.; Sköld, K. Boron neutron capture therapy for glioblastoma multiforme: clinical studies in Sweden. *J. neuro-oncology* **2003**, *62*, 135–144.
(35) Wang, Y.; Shao, G.; Wu, J.; Cui, C.; Zang, S.; Qiu, F.; Jia, R.; Wang, Z.; Wang, F. Preparation of ^{68}Ga-PSMA-11 with a synthesis module for micro PET-CT imaging of PSMA expression during prostate cancer progression. *Contrast Media Mol. Imaging* **2018,** 1-9.
(36) Moon, S. H.; Hong, M. K.; Kim, Y. J.; Lee, Y. S.; Lee, D. S.; Chung, J. K.; Jeong, J. M. Development of a Ga-68 labeled PET tracer with short linker for prostate-specific membrane antigen (PSMA) targeting. *Bioorganic Med. Chem.* **2018**, *26*, 2501–2507.
(37) Kozikowski, A. P.; Nan, F.; Conti, P.; Zhang, J.; Ramadan, E.; Bzdega, T.; Wroblewska, B.; Neale, J. H.; Pshenichkin, S.; Wroblewski, J. T. Design of remarkably simple, yet potent urea-based inhibitors of glutamate carboxypeptidase II (NAALADase). *J. Med. Chem.* **2001**, *44*, 298–

301.
(38) Banerjee, S. R.; Foss, C. A.; Castanares, M.; Mease, R. C.; Byun, Y.; Fox, J. J.; Hilton, J.; Lupold, S. E.; Kozikowski, A. P.; Pomper, M. G. Synthesis and evaluation of technetium-99m- and rhenium-labeled inhibitors of the prostate-specific membrane antigen (PSMA). *J. Med. Chem.* **2008**, *51*, 4504–4517.
(39) Barrett, J. A.; Babich, J. W.; Zimmerman, C. N.; Maresca, K. P.; Hillier, S. M.; Eckelman, W. C.; Barone, C.; Femia, F. J.; Keith, D.; Joyal, J. L.; Zimmerman, C. N.; Kozikowski, A. P.; Barrett, J. A.; Eckelman, W. C.; Babich, J. W. A series of halogenated heterodimeric inhibitors of prostate specific membrane antigen (PSMA) as radiolabeled probes for targeting prostate cancer. *J. Med. Chem.* **2008**, *52*, 347–357.
(40) Iguchi, Y.; Michiue, H.; Kitamatsu, M.; Hayashi, Y.; Takenaka, F.; Nishiki, T.; Matsui, H. Tumor-specific delivery of BSH-3R for boron neutron capture therapy and positron emission tomography imaging in a mouse brain tumor model. *Biomaterials* **2015**, *56*, 10–17.
(41) Geninatti-Crich, S.; Alberti, D.; Szabo, I.; Deagostino, A.; Toppino, A.; Barge, A.; Ballarini, F.; Bortolussi, S.; Bruschi, P.; Protti, N.; Stella, S.; Altieri, S.; Venturello, P.; Aime, S. MRI-guided neutron capture therapy by use of a dual gadolinium/boron agent targeted at tumour cells through upregulated low-density lipoprotein transporters. *Chem. - A Eur. J.* **2011**, *17*, 8479–8486.
(42) Evangelista, L.; Jori, G.; Martini, D.; Sotti, G. Boron neutron capture therapy and ^{18}F-labelled borophenylalanine positron emission tomography: A critical and clinical overview of the literature. *Applied Radiation and Isotopes*. **2013**, 91-101.
(43) Carpano, M.; Perona, M.; Rodriguez, C.; Nievas, S.; Olivera, M.; Santa Cruz, G. A.; Brandizzi, D.; Cabrini, R.; Pisarev, M.; Juvenal, G. J.; Dagrosa, M. A. Experimental studies of boronophenylalanine (^{10}BPA) biodistribution for the individual application of boron neutron capture therapy (BNCT) for malignant melanoma treatment. *Int. J. Radiat. Oncol. Biol. Phys.* **2015**. *93*, 344-352.
(44) Coderre, J. a; Glass, J. D.; Fairchild, R. G.; Micca, P. L.; Fand, I.; Joel, D. D. Selective delivery of boron by the melanin precursor analogue p-boronophenylalanine to tumors other than melanoma. *Cancer Res.* **1990**, *50*, 138–141.
(45) Wu, G.; Yang, W.; Barth, R. F.; Kawabata, S.; Swindall, M.; Bandyopadhyaya, A. K.; Tjarks, W.; Khorsandi, B.; Blue, T. E.; Ferketich, A. K.; Yang, M.; Christoforidis, G. A.; Sferra, T. J.; Binns, P. J.; Riley, K. J.; Ciesielski, M. J.; Fenstermaker, R. A. Molecular targeting and treatment of an epidermal growth factor receptor-positive glioma using boronated Cetuximab. *Clin. Cancer Res.* **2007**, *13*, 1260–1268.
(46) Takeuchi, I.; Nomura, K.; Makino, K. Hydrophobic boron compound-loaded poly(*L*-lactide-co-glycolide) nanoparticles for boron neutron capture therapy. *Colloids Surfaces B Biointerfaces* **2017,** *159*, 360-365.
(47) Sumitani, S.; Nagasaki, Y. Boron neutron capture therapy assisted by boron-conjugated nanoparticles. *Polymer Journal*. **2012**, *44*, 522-530.
(48) Oleshkevich, E.; Morancho, A.; Saha, A.; Galenkamp, K. M. O.; Grayston, A.; Crich, S. G.; Alberti, D.; Protti, N.; Comella, J. X.; Teixidor, F.; Rosell, A.; Viñas, C. Combining magnetic nanoparticles and icosahedral boron clusters in biocompatible inorganic nanohybrids for cancer therapy. *Nanomedicine Nanotechnology, Biol. Med.* **2019**, *20*, 101986.
(49) Hey-Hawkins, E.; Viñas-Teixidor, C. Boron-based compounds: potential and emerging applications in medicine. John Wiley & Sons, Ltd, Hoboken, NJ, USA, 2018.
(50) Taylor, R. M.; Severns, V.; Brown, D. C.; Bisoffi, M.; Sillerud, L. O. Prostate cancer targeting motifs: expression of $\alpha_v\beta_3$, neurotensin receptor 1, prostate specific membrane antigen,

and prostate stem cell antigen in human prostate cancer cell lines and xenografts. *Prostate* **2012**, *72*, 523–532.

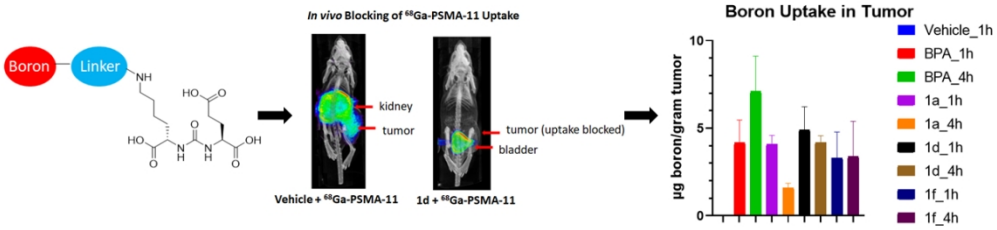
Boron
Linker
NH
HO
O
HO
O
N
H
N
H
OH
O
O
In vivo Blocking of 68Ga-PSMA-11 Uptake
kidney
tumor
tumor (uptake blocked)
bladder
Vehicle + 68Ga-PSMA-11
1d + 68Ga-PSMA-11
Boron Uptake in Tumor
μg boron/gram tumor
10
5
0
Vehicle_1h
BPA_1h
BPA_4h
1a_1h
1a_4h
1d_1h
1d_4h
1f_1h
1f_4h

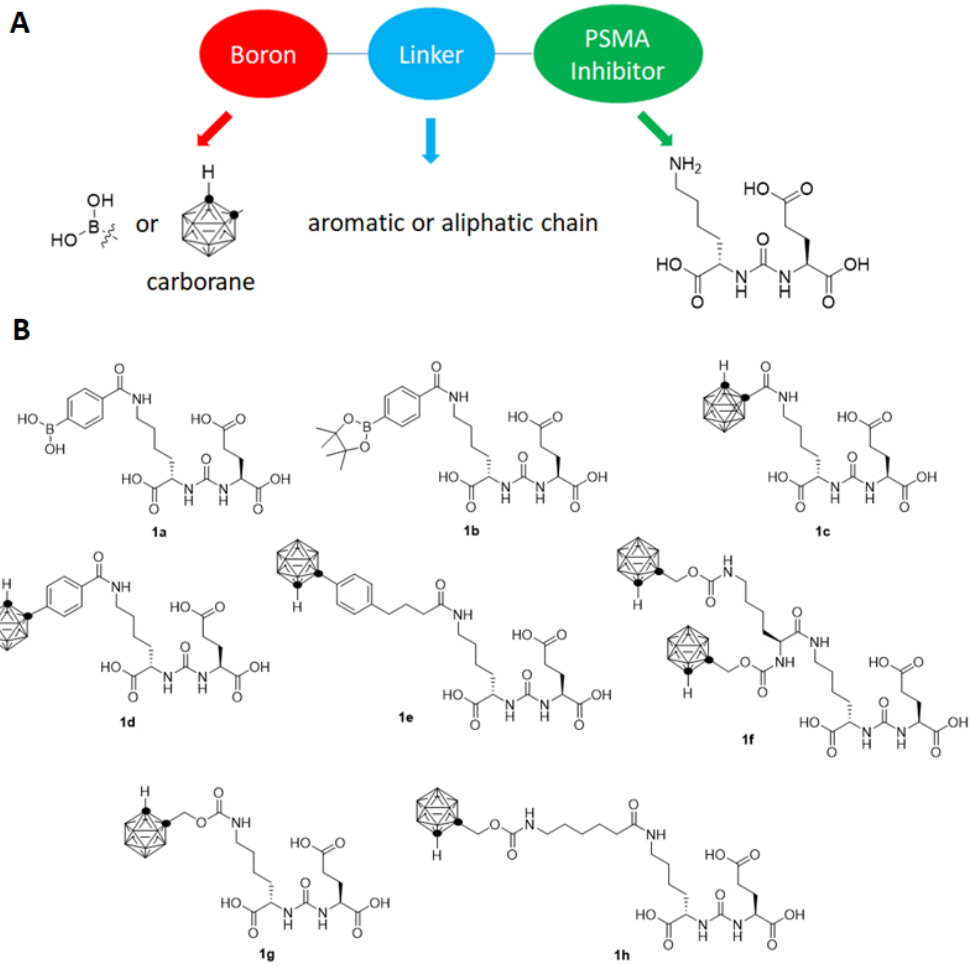

Figure 1. (A) The design of boron labeled PSMA targeted agents includes a urea based inhibitory element, connected to a boron containing substituent via a linker moiety. (B) Structures of boron labeled PSMA agents evaluated in this study.

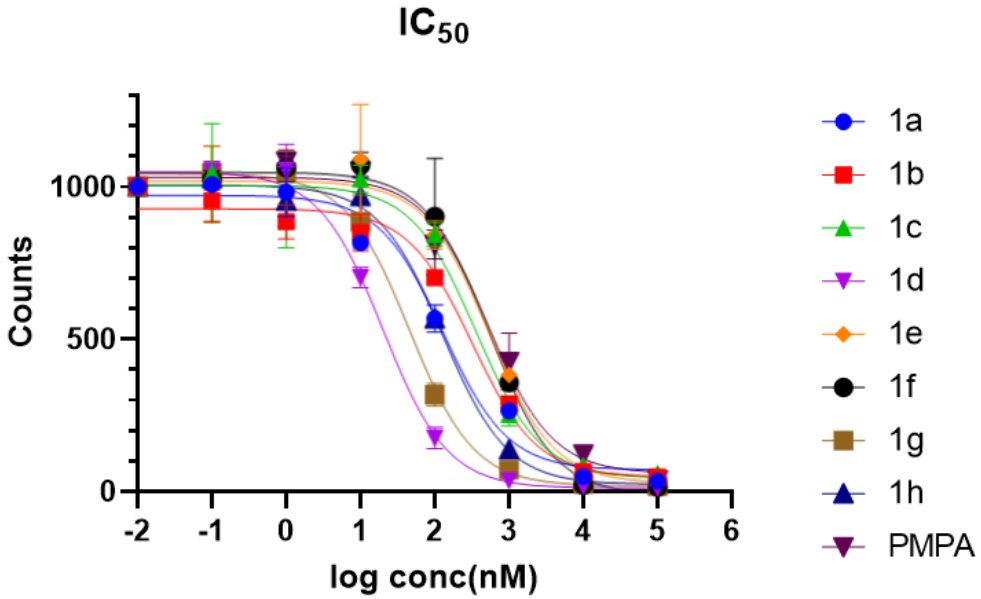

Figure 2. IC50 of compounds 1a-1h determined by a competitive binding assay against 68Ga-PSMA-11 on PSMA expressing 22Rv1 cells.

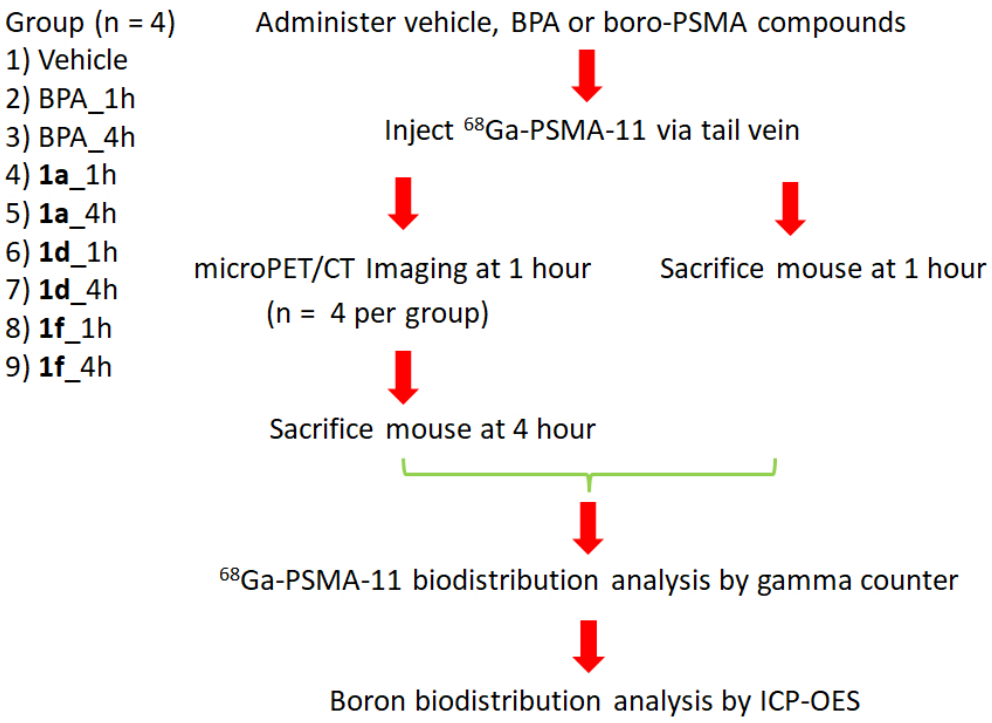

Figure 3. Flow chart of PET imaging, 68Ga-PSMA-11 biodistribution and boron biodistribution assay performed in mice bearing 22Rv1 xenograft tumors.

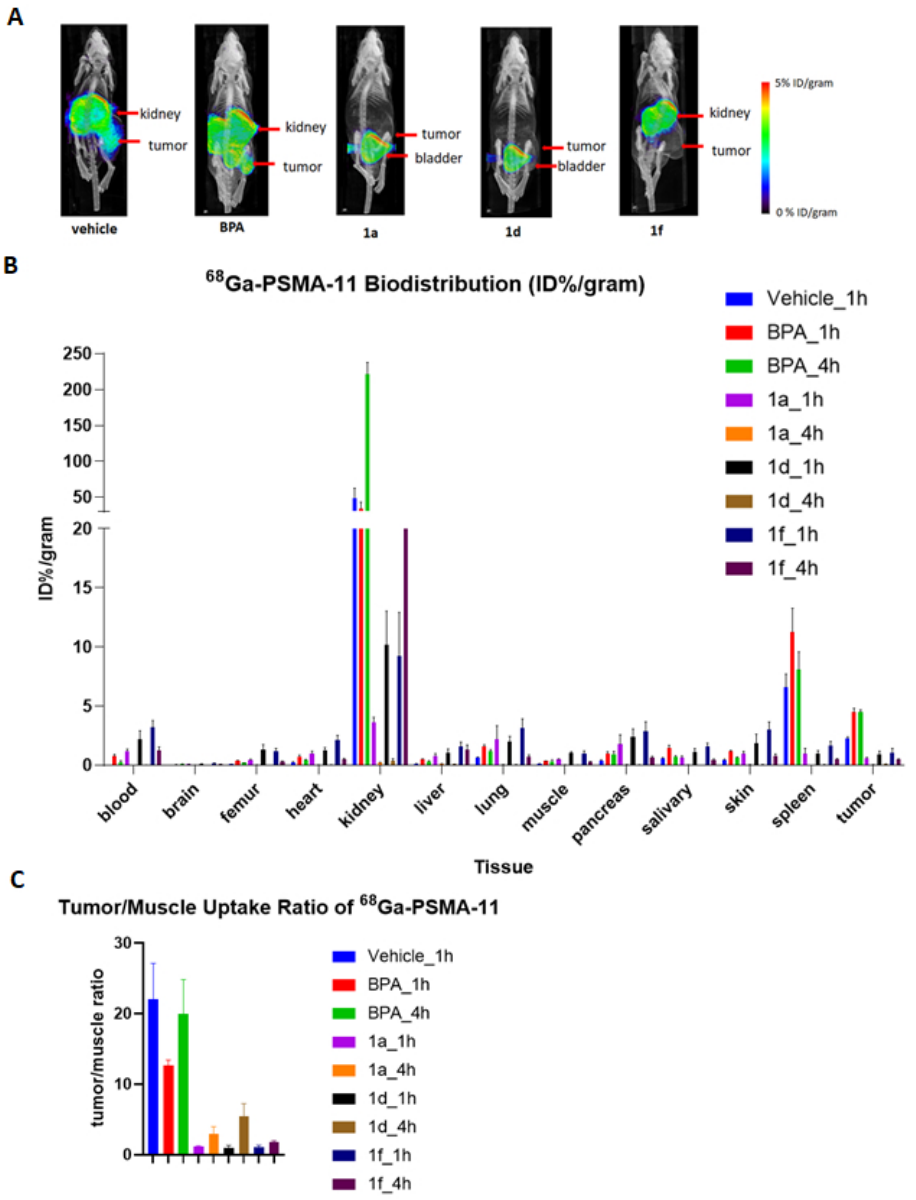

Figure 4. (A) PET imaging results showed efficient blocking of 68Ga-PSMA-11 uptake by boro-PSMA compounds, but not by BPA. (B) 68Ga-PSMA-11 biodistribution as determined by collection of organs and gamma counting. (C) Tumor/muscle uptake ratio of 68Ga-PSMA-11.

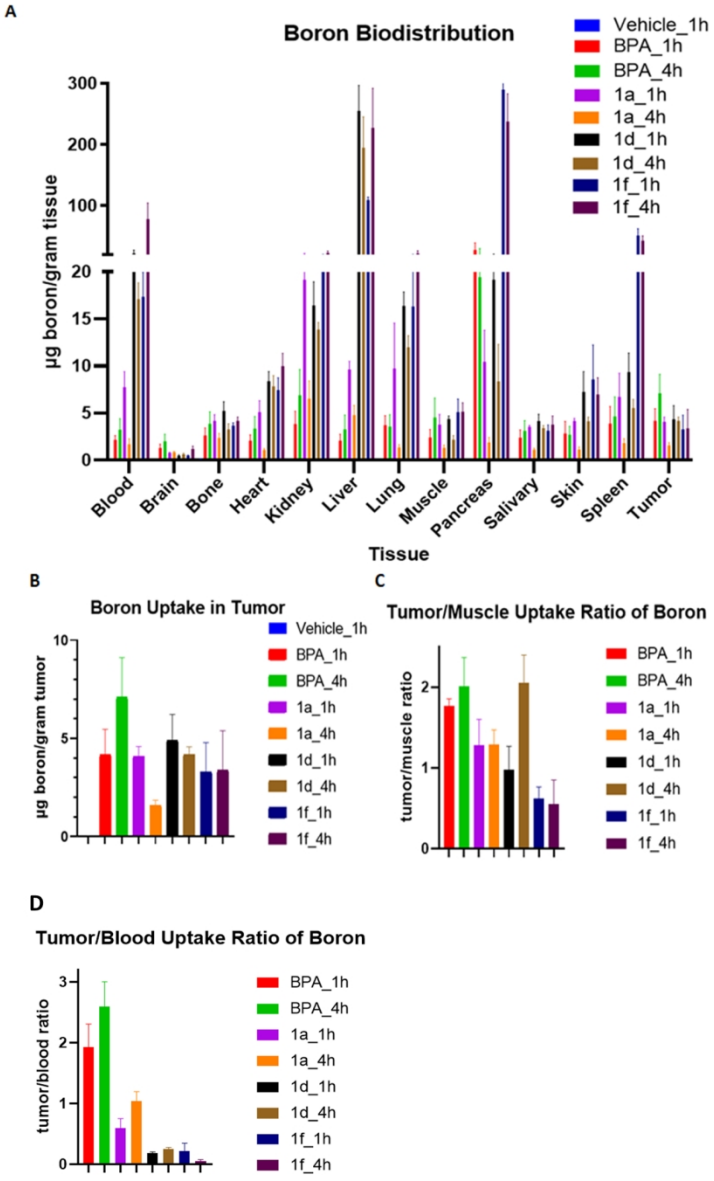

Figure 5. (A) Boron biodistribution. Tissues were harvested as indicated in figure 3, homogenized and boron content was determined by ICP-OES. (B) Boron uptake in tumor (C) Tumor/muscle uptake ratio of boron. (D) Tumor/blood uptake ratio of boron.

381x571mm (96 x 96 DPI)